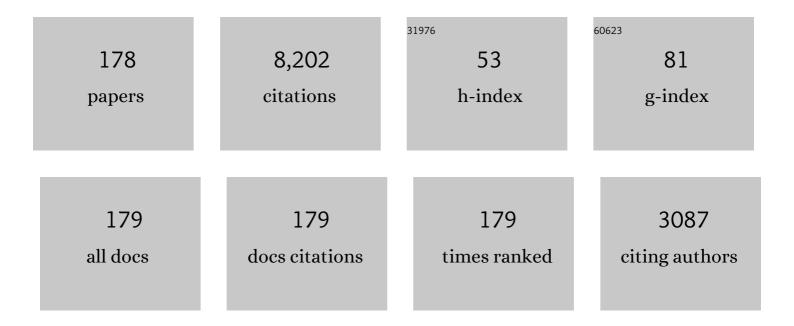
Thomas Pütterich

List of Publications by Year in descending order

Source: https://exaly.com/author-pdf/6457027/publications.pdf Version: 2024-02-01



ΤΗΟΜΛΟ ΡΑΊ/ ΤΤΕΡΙΟΗ

#	Article	IF	CITATIONS
1	First Observation of Edge Localized Modes Mitigation with Resonant and Nonresonant Magnetic Perturbations in ASDEX Upgrade. Physical Review Letters, 2011, 106, 225004.	7.8	428
2	Modelling of measured tungsten spectra from ASDEX Upgrade and predictions for ITER. Plasma Physics and Controlled Fusion, 2008, 50, 085016.	2.1	259
3	Tungsten: an option for divertor and main chamber plasma facing components in future fusion devices. Nuclear Fusion, 2005, 45, 209-218.	3.5	209
4	Calculation and experimental test of the cooling factor of tungsten. Nuclear Fusion, 2010, 50, 025012.	3.5	189
5	Divertor power load feedback with nitrogen seeding in ASDEX Upgrade. Plasma Physics and Controlled Fusion, 2010, 52, 055002.	2.1	173
6	Overview on plasma operation with a full tungsten wall in ASDEX Upgrade. Journal of Nuclear Materials, 2013, 438, S34-S41.	2.7	156
7	Overview of the JET results in support to ITER. Nuclear Fusion, 2017, 57, 102001.	3.5	150
8	Plasma-wall interaction and plasma behaviour in the non-boronised all tungsten ASDEX Upgrade. Journal of Nuclear Materials, 2009, 390-391, 858-863.	2.7	142
9	Tungsten transport in JET H-mode plasmas in hybrid scenario, experimental observations and modelling. Nuclear Fusion, 2014, 54, 083028.	3.5	139
10	High-accuracy characterization of the edge radial electric field at ASDEX Upgrade. Nuclear Fusion, 2013, 53, 053005.	3.5	117
11	Plasma surface interactions in impurity seeded plasmas. Journal of Nuclear Materials, 2011, 415, S19-S26.	2.7	116
12	Tungsten divertor erosion in all metal devices: Lessons from the ITER like wall of JET. Journal of Nuclear Materials, 2013, 438, S42-S47.	2.7	116
13	Plasma wall interaction and its implication in an all tungsten divertor tokamak. Plasma Physics and Controlled Fusion, 2007, 49, B59-B70.	2.1	110
14	High-resolution charge exchange measurements at ASDEX Upgrade. Review of Scientific Instruments, 2012, 83, 103501.	1.3	109
15	DEMO divertor limitations during and in between ELMs. Nuclear Fusion, 2014, 54, 114003.	3.5	107
16	Theoretical description of heavy impurity transport and its application to the modelling of tungsten in JET and ASDEX upgrade. Plasma Physics and Controlled Fusion, 2015, 57, 014031.	2.1	107
17	Tokamak operation with high-Zplasma facing components. Plasma Physics and Controlled Fusion, 2005, 47, B207-B222.	2.1	102
18	ELM-free stationary H-mode plasmas in the ASDEX Upgrade tokamak. Plasma Physics and Controlled Fusion, 2003, 45, 1399-1416.	2.1	99

2

Thomas Pütterich

#	Article	IF	CITATIONS
19	Intrinsic Toroidal Rotation, Density Peaking, and Turbulence Regimes in the Core of Tokamak Plasmas. Physical Review Letters, 2011, 107, 215003.	7.8	99
20	Non-boronized compared with boronized operation of ASDEX Upgrade with full-tungsten plasma facing components. Nuclear Fusion, 2009, 49, 045007.	3.5	98
21	H-mode threshold and confinement in helium and deuterium in ASDEX Upgrade. Nuclear Fusion, 2009, 49, 062003.	3.5	98
22	Power exhaust by SOL and pedestal radiation at ASDEX Upgrade and JET. Nuclear Materials and Energy, 2017, 12, 111-118.	1.3	92
23	Plasma shut-down with fast impurity puff on ASDEX Upgrade. Nuclear Fusion, 2007, 47, 023.	3.5	88
24	Confinement of â€~improved H-modes' in the all-tungsten ASDEX Upgrade with nitrogen seeding. Nuclear Fusion, 2011, 51, 113003.	3.5	84
25	The physics and technology basis entering European system code studies for DEMO. Nuclear Fusion, 2017, 57, 016011.	3.5	84
26	ELM-induced transient tungsten melting in the JET divertor. Nuclear Fusion, 2015, 55, 023010.	3.5	83
27	Disentangling the emissions of highly ionized tungsten in the range 4–14 nm. Journal of Physics B: Atomic, Molecular and Optical Physics, 2005, 38, 3071-3082.	1.5	81
28	Observations on the W-transport in the core plasma of JET and ASDEX Upgrade. Plasma Physics and Controlled Fusion, 2013, 55, 124036.	2.1	81
29	Final steps to an all tungsten divertor tokamak. Journal of Nuclear Materials, 2007, 363-365, 52-59.	2.7	80
30	L- to H-mode transitions at low density in ASDEX Upgrade. Nuclear Fusion, 2012, 52, 012001.	3.5	80
31	Gyrokinetic modelling of electron and boron density profiles of H-mode plasmas in ASDEX Upgrade. Nuclear Fusion, 2011, 51, 023006.	3.5	75
32	Spectroscopy of highly charged tungsten ions relevant to fusion plasmas. Physica Scripta, 2009, T134, 014026.	2.5	73
33	Efficient generation of energetic ions in multi-ion plasmas by radio-frequency heating. Nature Physics, 2017, 13, 973-978.	16.7	73
34	Studies of edge localized mode mitigation with new active in-vessel saddle coils in ASDEX Upgrade. Plasma Physics and Controlled Fusion, 2011, 53, 124014.	2.1	71
35	Assessment of compatibility of ICRF antenna operation with full W wall in ASDEX Upgrade. Nuclear Fusion, 2010, 50, 035004.	3.5	71
36	Overview of the JET results with the ITER-like wall. Nuclear Fusion, 2013, 53, 104002.	3.5	70

#	Article	IF	CITATIONS
37	Compatibility of ITER scenarios with full tungsten wall in ASDEX Upgrade. Nuclear Fusion, 2009, 49, 115014.	3.5	68
38	Evidence for the neoclassical nature of the radial electric field in the edge transport barrier of ASDEX Upgrade. Nuclear Fusion, 2014, 54, 012003.	3.5	66
39	ELM flushing and impurity transport in the H-mode edge barrier in ASDEX Upgrade. Journal of Nuclear Materials, 2011, 415, S334-S339.	2.7	64
40	Progress at JET in integrating ITER-relevant core and edge plasmas within the constraints of an ITER-like wall. Plasma Physics and Controlled Fusion, 2015, 57, 035004.	2.1	64
41	Evidence for Strong Inversed Shear of Toroidal Rotation at the Edge-Transport Barrier in the ASDEX Upgrade. Physical Review Letters, 2009, 102, 025001.	7.8	63
42	The influence of an ITER-like wall on disruptions at JET. Physics of Plasmas, 2014, 21, .	1.9	61
43	Ten years of W programme in ASDEX Upgrade—challenges and conclusions. Physica Scripta, 2009, T138, 014038.	2.5	60
44	ICRF operation with improved antennas in ASDEX Upgrade with W wall. Nuclear Fusion, 2013, 53, 093018.	3.5	60
45	Core intrinsic rotation behaviour in ASDEX Upgrade ohmic L-mode plasmas. Nuclear Fusion, 2014, 54, 043009.	3.5	60
46	ELM-resolved divertor erosion in the JET ITER-Like Wall. Nuclear Fusion, 2016, 56, 026014.	3.5	60
47	Determination of the tolerable impurity concentrations in a fusion reactor using a consistent set of cooling factors. Nuclear Fusion, 2019, 59, 056013.	3.5	60
48	First scenario development with the JET new ITER-like wall. Nuclear Fusion, 2014, 54, 013011.	3.5	59
49	Optimization of ICRH for core impurity control in JET-ILW. Nuclear Fusion, 2016, 56, 036022.	3.5	59
50	Making ICRF power compatible with a high-Z wall in ASDEX Upgrade. Plasma Physics and Controlled Fusion, 2017, 59, 014022.	2.1	59
51	First operation with the JET International Thermonuclear Experimental Reactor-like wall. Physics of Plasmas, 2013, 20, .	1.9	56
52	Main chamber sources and edge transport of tungsten in H-mode plasmas at ASDEX Upgrade. Nuclear Fusion, 2011, 51, 053002.	3.5	55
53	First results with 3-strap ICRF antennas in ASDEX Upgrade. Nuclear Fusion, 2016, 56, 084001.	3.5	54
54	Edge transport and its interconnection with main chamber recycling in ASDEX Upgrade. Nuclear Fusion, 2003, 43, 573-578.	3.5	53

#	Article	IF	CITATIONS
55	Estimation of profiles of the effective ion charge at ASDEX Upgrade with Integrated Data Analysis. Plasma Physics and Controlled Fusion, 2010, 52, 095008.	2.1	53
56	ELM induced tungsten melting and its impact on tokamak operation. Journal of Nuclear Materials, 2015, 463, 78-84.	2.7	53
57	Overview of ASDEX Upgrade results. Nuclear Fusion, 2017, 57, 102015.	3.5	53
58	Particle and impurity transport in the Axial Symmetric Divertor Experiment Upgrade and the Joint European Torus, experimental observations and theoretical understanding. Physics of Plasmas, 2007, 14, 055905.	1.9	52
59	Local effects of ECRH on argon transport in L-mode discharges at ASDEX Upgrade. Plasma Physics and Controlled Fusion, 2011, 53, 035024.	2.1	51
60	I-mode studies at ASDEX Upgrade: L-I and I-H transitions, pedestal and confinement properties. Nuclear Fusion, 2017, 57, 016004.	3.5	51
61	Tungsten erosion at the ICRH limiters in ASDEX Upgrade. Journal of Nuclear Materials, 2007, 363-365, 112-116.	2.7	50
62	Overview of the JET results. Nuclear Fusion, 2015, 55, 104001.	3.5	50
63	The impact of poloidal asymmetries on tungsten transport in the core of JET H-mode plasmas. Physics of Plasmas, 2015, 22, 055902.	1.9	49
64	Integrated exhaust control with divertor parameter feedback and pellet ELM pacemaking in ASDEX Upgrade. Journal of Nuclear Materials, 2005, 337-339, 732-736.	2.7	48
65	First EMC3-Eirene simulations of the impact of the edge magnetic perturbations at ASDEX Upgrade compared with the experiment. Nuclear Fusion, 2012, 52, 054013.	3.5	47
66	Integrated exhaust scenarios with actively controlled ELMs. Nuclear Fusion, 2005, 45, 502-511.	3.5	46
67	Effect of electron cyclotron resonance heating (ECRH) on toroidal rotation in ASDEX Upgrade H-mode discharges. Plasma Physics and Controlled Fusion, 2011, 53, 035007.	2.1	46
68	Operational conditions in a W-clad tokamak. Journal of Nuclear Materials, 2007, 367-370, 1497-1502.	2.7	45
69	Core momentum and particle transport studies in the ASDEX Upgrade tokamak. Plasma Physics and Controlled Fusion, 2011, 53, 124013.	2.1	45
70	Poloidal asymmetry of parallel rotation measured in ASDEX Upgrade. Nuclear Fusion, 2012, 52, 083013.	3.5	44
71	Study of quiescent H-mode plasmas in ASDEX Upgrade. Plasma Physics and Controlled Fusion, 2004, 46, A151-A156.	2.1	43
72	Magnetic structure and frequency scaling of limit-cycle oscillations close to L- to H-mode transitions. Nuclear Fusion, 2016, 56, 086009.	3.5	43

#	Article	IF	CITATIONS
73	Extensions to the charge exchange recombination spectroscopy diagnostic suite at ASDEX Upgrade. Review of Scientific Instruments, 2017, 88, 073508.	1.3	43
74	Interplay between turbulence, neoclassical and zonal flows during the transition from low to high confinement mode at ASDEX Upgrade. Nuclear Fusion, 2017, 57, 014002.	3.5	40
75	Characterization of edge profiles and fluctuations in discharges with type-II and nitrogen-mitigated edge localized modes in ASDEX Upgrade. Plasma Physics and Controlled Fusion, 2011, 53, 085026.	2.1	39
76	Overview of physics studies on ASDEX Upgrade. Nuclear Fusion, 2019, 59, 112014.	3.5	38
77	Observation of anomalous impurity transport during low-density experiments in W7-X with laser blow-off injections of iron. Nuclear Fusion, 2019, 59, 046009.	3.5	38
78	The role of MHD in causing impurity peaking in JET hybrid plasmas. Nuclear Fusion, 2016, 56, 066002.	3.5	37
79	Overview of ASDEX Upgrade results. Nuclear Fusion, 2013, 53, 104003.	3.5	36
80	L-H transition physics in hydrogen and deuterium: key role of the edge radial electric field and ion heat flux. Plasma Physics and Controlled Fusion, 2016, 58, 014007.	2.1	36
81	Long-term evolution of the impurity composition and impurity events with the ITER-like wall at JET. Nuclear Fusion, 2013, 53, 073043.	3.5	35
82	ICRF specific plasma wall interactions in JET with the ITER-like wall. Journal of Nuclear Materials, 2013, 438, S160-S165.	2.7	35
83	Connecting the global H-mode power threshold to the local radial electric field at ASDEX Upgrade. Nuclear Fusion, 2020, 60, 066026.	3.5	35
84	Induced tungsten melting events in the divertor of ASDEX Upgrade and their influence on plasma performance. Journal of Nuclear Materials, 2011, 415, S297-S300.	2.7	34
85	Filament transport, warm ions and erosion in ASDEX Upgrade L-modes. Nuclear Fusion, 2015, 55, 033018.	3.5	34
86	Overview of JET results. Nuclear Fusion, 2011, 51, 094008.	3.5	33
87	Tungsten impurity transport experiments in Alcator C-Mod to address high priority research and	1.9	33
88	Optimized tomography methods for plasma emissivity reconstruction at the ASDEX Upgrade tokamak. Review of Scientific Instruments, 2016, 87, 123505.	1.3	32
89	lon cyclotron resonance heating for tungsten control in various JET H-mode scenarios. Plasma Physics and Controlled Fusion, 2017, 59, 055001.	2.1	32
90	Analysis of temperature and density pedestal gradients in AUG, DIII-D and JET. Nuclear Fusion, 2013, 53, 073039.	3.5	31

#	Article	IF	CITATIONS
91	Modification of impurity transport in the presence of saturated (<i>m</i> , <i>n</i>) = (1,1) MHD activity at ASDEX Upgrade. Plasma Physics and Controlled Fusion, 2015, 57, 075004.	2.1	31
92	Rotation and density asymmetries in the presence of large poloidal impurity flows in the edge pedestal. Plasma Physics and Controlled Fusion, 2013, 55, 124037.	2.1	30
93	A comparison of the impact of central ECRH and central ICRH on the tungsten behaviour in ASDEX Upgrade H-mode plasmas. Nuclear Fusion, 2017, 57, 056015.	3.5	30
94	The role of the source versus the collisionality in predicting a reactor density profile as observed on ASDEX Upgrade discharges. Nuclear Fusion, 2019, 59, 076042.	3.5	30
95	Experiences With Tungsten Plasma Facing Components in ASDEX Upgrade and JET. IEEE Transactions on Plasma Science, 2014, 42, 552-562.	1.3	29
96	Tungsten transport and sources control in JET ITER-like wall H-mode plasmas. Journal of Nuclear Materials, 2015, 463, 85-90.	2.7	29
97	Overview of ASDEX Upgrade results—development of integrated operating scenarios for ITER. Nuclear Fusion, 2005, 45, S98-S108.	3.5	28
98	Pedestal and <i>E</i> _r profile evolution during an edge localized mode cycle at ASDEX Upgrade. Plasma Physics and Controlled Fusion, 2017, 59, 105007.	2.1	28
99	Overview of ASDEX Upgrade results. Nuclear Fusion, 2011, 51, 094012.	3.5	27
100	Stationary ELM-free H-mode in ASDEX Upgrade. Nuclear Fusion, 2020, 60, 054003.	3.5	27
101	Assessment of the baseline scenario at <i>q</i> ₉₅ ~ 3 for ITER. Nuclear Fusion, 2018, 58, 126010.	3.5	26
102	Plasma surface interaction with tungsten in ASDEX Upgrade. Journal of Nuclear Materials, 2005, 337-339, 852-856.	2.7	25
103	Controlled tungsten melting and droplet ejection studies in ASDEX Upgrade. Physica Scripta, 2011, T145, 014067.	2.5	25
104	Development of the gas puff charge exchange recombination spectroscopy (GP-CXRS) technique for ion measurements in the plasma edge. Review of Scientific Instruments, 2013, 84, 093505.	1.3	25
105	Investigation of inter-ELM pedestal profiles in ASDEX Upgrade. Plasma Physics and Controlled Fusion, 2009, 51, 124057.	2.1	24
106	ICRF antenna-plasma interactions and its influence on W sputtering in ASDEX upgrade. Journal of Nuclear Materials, 2011, 415, S1005-S1008.	2.7	24
107	Investigation of inter-ELM ion heat transport in the H-mode pedestal of ASDEX Upgrade plasmas. Nuclear Fusion, 2017, 57, 022020.	3.5	24
108	H-mode power threshold studies in mixed ion species plasmas at ASDEX Upgrade. Nuclear Fusion, 2020, 60, 074001.	3.5	24

#	Article	IF	CITATIONS
109	Influence of gas injection location and magnetic perturbations on ICRF antenna performance in ASDEX Upgrade. , 2014, , .		23
110	Overview of progress in European medium sized tokamaks towards an integrated plasma-edge/wall solution ^a . Nuclear Fusion, 2017, 57, 102014.	3.5	23
111	L–H transition in the presence of magnetic perturbations in ASDEX Upgrade. Nuclear Fusion, 2012, 52, 114014.	3.5	22
112	Determination of tungsten and molybdenum concentrations from an x-ray range spectrum in JET with the ITER-like wall configuration. Journal of Physics B: Atomic, Molecular and Optical Physics, 2015, 48, 144023.	1.5	22
113	Measurement of the complete core plasma flow across the LOC–SOC transition at ASDEX Upgrade. Nuclear Fusion, 2018, 58, 026013.	3.5	22
114	Evolution of nitrogen concentration and ammonia production in N ₂ -seeded H-mode discharges at ASDEX Upgrade. Nuclear Fusion, 2019, 59, 046010.	3.5	22
115	A fast edge charge exchange recombination spectroscopy system at the ASDEX Upgrade tokamak. Review of Scientific Instruments, 2017, 88, 043103.	1.3	21
116	Carbon erosion and a:C–H layer formation at ASDEX Upgrade. Journal of Nuclear Materials, 2005, 337-339, 847-851.	2.7	20
117	Investigation of passive edge emission in charge exchange spectra at the ASDEX Upgrade tokamak. Plasma Physics and Controlled Fusion, 2011, 53, 035002.	2.1	20
118	Observation of different phases during an ELM crash with the help of nitrogen seeding. Plasma Physics and Controlled Fusion, 2014, 56, 025011.	2.1	20
119	The physics of W transport illuminated by recent progress in W density diagnostics at ASDEX Upgrade. Plasma Physics and Controlled Fusion, 2018, 60, 014003.	2.1	20
120	Spectroscopic investigation of carbon migration with tungsten walls in ASDEX Upgrade. Journal of Nuclear Materials, 2007, 363-365, 60-65.	2.7	19
121	Mitigation of edge localised modes with magnetic perturbations in ASDEX Upgrade. Fusion Engineering and Design, 2013, 88, 446-453.	1.9	19
122	Core transport analysis of nitrogen seeded H-mode discharges in the ASDEX Upgrade. Plasma Physics and Controlled Fusion, 2013, 55, 015010.	2.1	19
123	Impact of W events and dust on JET-ILW operation. Journal of Nuclear Materials, 2015, 463, 837-841.	2.7	19
124	Optimization of the computation of total and local radiated power at ASDEX Upgrade. Nuclear Fusion, 2021, 61, 066025.	3.5	19
125	Carbon influx studies in the main chamber of ASDEX Upgrade. Plasma Physics and Controlled Fusion, 2003, 45, 1873-1892.	2.1	18
126	Carbon Erosion and Migration in Fusion Devices. Physica Scripta, 2004, T111, 55.	2.5	18

8

THOMAS PÃ¹/4TTERICH

#	Article	IF	CITATIONS
127	Collisionality dependence of edge rotation and in–out impurity asymmetries in ASDEX Upgrade H-mode plasmas. Nuclear Fusion, 2015, 55, 123002.	3.5	18
128	Understanding helium transport: experimental and theoretical investigations of low-Z impurity transport at ASDEX Upgrade. Nuclear Fusion, 2019, 59, 056014.	3.5	18
129	The ASDEX Upgrade divertor Ilb—a closed divertor for strongly shaped plasmas. Nuclear Fusion, 2003, 43, 1191-1196.	3.5	17
130	Compatibility of ICRF antennas with W-coated limiters for different plasma geometries in ASDEX Upgrade. Journal of Nuclear Materials, 2007, 363-365, 122-126.	2.7	17
131	Operation of ICRF antennas in a full tungsten environment in ASDEX Upgrade. Journal of Nuclear Materials, 2009, 390-391, 900-903.	2.7	17
132	Ion cyclotron resonance frequency heating in JET during initial operations with the ITER-like wall. Physics of Plasmas, 2014, 21, 061510.	1.9	16
133	The local nature of the plasma response to cold pulses with electron and ion heating at ASDEX Upgrade. Nuclear Fusion, 2019, 59, 106007.	3.5	16
134	Exploring fusion-reactor physics with high-power electron cyclotron resonance heating on ASDEX Upgrade. Plasma Physics and Controlled Fusion, 2020, 62, 024012.	2.1	16
135	3D modeling of the ASDEX Upgrade edge plasma exposed to a localized tungsten source by means of EMC3-Eirene. Journal of Nuclear Materials, 2011, 415, S505-S508.	2.7	15
136	Development of the Q  =  10 scenario for ITER on ASDEX Upgrade (AUG). Nuclear Fusion, 202	16, 5 65, 106	500175
137	Validation of quasi-linear turbulent transport models against plasmas with dominant electron heating for the prediction of ITER PFPO-1 plasmas. Nuclear Fusion, 2021, 61, 066035.	3.5	15
138	Tungsten behaviour in radiatively cooled plasma discharges in ASDEX Upgrade. Journal of Nuclear Materials, 2011, 415, S322-S326.	2.7	14
139	Recent ASDEX Upgrade Results and Future Extension Plans. IEEE Transactions on Plasma Science, 2012, 40, 605-613.	1.3	13
140	Fast-ion pressure dominating the mass dependence of the core heat transport in ASDEX Upgrade H-modes. Nuclear Fusion, 2021, 61, 036033.	3.5	13
141	Development of Ar+16 charge exchange recombination spectroscopy measurements at ASDEX Upgrade. Nuclear Fusion, 2021, 61, 016019.	3.5	12
142	Material Transport in ASDEX Upgrade. Physica Scripta, 2004, T111, 49.	2.5	11
143	Overview of ASDEX Upgrade results. Nuclear Fusion, 2009, 49, 104009.	3.5	11
144	Parameter dependence of the radial electric field in the edge pedestal of hydrogen, deuterium and helium plasmas. Plasma Physics and Controlled Fusion, 2014, 56, 075018.	2.1	11

#	Article	IF	CITATIONS
145	On the challenge of plasma heating with the JET metallic wall. Nuclear Fusion, 2014, 54, 033002.	3.5	11
146	Progress in reducing ICRF-specific impurity release in ASDEX upgrade and JET. Nuclear Materials and Energy, 2017, 12, 1194-1198.	1.3	11
147	Interaction of ICRF Fields with the Plasma Boundary in AUG and JET and Guidelines for Antenna Optimization. , 2009, , .		10
148	Progress in characterization and modelling of the current ramp-up phase of ASDEX Upgrade discharges. Nuclear Fusion, 2012, 52, 063017.	3.5	10
149	The upgraded ASDEX Upgrade contribution to the ITPA confinement database: description and analysis. Nuclear Fusion, 2021, 61, 046030.	3.5	10
150	The dependence of confinement on the isotope mass in the core and the edge of AUG and JET-ILW H-mode plasmas. Nuclear Fusion, 2022, 62, 026014.	3.5	10
151	3D trajectories re-construction of droplets ejected in controlled tungsten melting studies in ASDEX Upgrade. Journal of Nuclear Materials, 2013, 438, S846-S851.	2.7	9
152	Investigation of 3D tungsten distributions in (1,1) kink modes induced by toroidal plasma rotation. Plasma Physics and Controlled Fusion, 2015, 57, 085002.	2.1	9
153	Experimental inference of neutral and impurity transport in Alcator C-Mod using high-resolution x-ray and ultra-violet spectra. Nuclear Fusion, 2021, 61, 126060.	3.5	8
154	Recent progress in understanding the L–H transition physics from ASDEX Upgrade. Plasma Physics and Controlled Fusion, 2012, 54, 124002.	2.1	7
155	The extreme ultraviolet emissions of W[sup 23+](4f[sup 5]). , 2013, , .		7
156	Optimisation and assessment of theoretical impurity line power coefficients relevant to ITER and DEMO. Plasma Physics and Controlled Fusion, 2017, 59, 055010.	2.1	7
157	Spectroscopic investigation of heavy impurity behaviour during ICRH with the JET ITER-like wall. , 2014, , \cdot		6
158	Impact of W on scenario simulations for ITER. Nuclear Fusion, 2015, 55, 063031.	3.5	6
159	I-mode in non-deuterium plasmas in ASDEX Upgrade. Nuclear Fusion, 2021, 61, 054001.	3.5	6
160	Soft X-ray tomographic reconstruction of JET ILW plasmas with tungsten impurity and different spectral response of detectors. Fusion Engineering and Design, 2015, 96-97, 869-872.	1.9	5
161	ITER-like current ramps in JET with ILW: experiments, modelling and consequences for ITER. Nuclear Fusion, 2015, 55, 013009.	3.5	5
162	Imaging motional Stark effect measurements at ASDEX Upgrade. Review of Scientific Instruments, 2016, 87, 11E537.	1.3	5

#	Article	IF	CITATIONS
163	Understanding of impurity poloidal distribution in the edge pedestal by modelling. Nuclear Fusion, 2015, 55, 073017.	3.5	4
164	CXRS measurements of energetic helium ions in ASDEX Upgrade plasmas heated with a 3-ion ICRF scenario. Nuclear Fusion, 2021, 61, 036017.	3.5	4
165	Simulation of edge radial electric fields in H-regimes of ASDEX-Upgrade. Journal of Nuclear Materials, 2011, 415, S593-S596.	2.7	3
166	Measurements and ERO simulations of carbon flows in the high-field side main SOL in AUG. Journal of Nuclear Materials, 2013, 438, S410-S413.	2.7	3
167	First analysis of tungsten transport in the edge of Tore Supra plasmas. Journal of Nuclear Materials, 2013, 438, S526-S529.	2.7	3
168	Effect of the minority concentration on ion cyclotron resonance heating in presence of the ITER-like wall in JET. , 2014, , .		3
169	ICRF heating in JET during initial operations with the ITER-like wall. , 2014, , .		3
170	Trends of W behavior in ICRF assisted discharges in ASDEX Upgrade. Journal of Nuclear Materials, 2015, 463, 601-604.	2.7	3
171	Dynamics of the pedestal transport during edge localized mode cycles at ASDEX Upgrade. Plasma Physics and Controlled Fusion, 2020, 62, 024009.	2.1	3
172	Comparison of ICRF and NBI heated plasmas performances in the JET ITER-like wall. , 2014, , .		2
173	Statistical comparison of ICRF and NBI heating performance in JET-ILW L-mode plasmas. , 2014, , .		2
174	Cascade emission in electron beam ion trap plasma of W25+ ion. Journal of Quantitative Spectroscopy and Radiative Transfer, 2015, 160, 22-28.	2.3	2
175	In-out charge exchange measurements and 3D modelling of diagnostic thermal neutrals to study edge poloidal impurity asymmetries. Plasma Physics and Controlled Fusion, 2022, 64, 045021.	2.1	2
176	Local 3D perturbation experiments for probing the ELM stability. European Physical Journal D, 2005, 55, 1557-1567.	0.4	1
177	Synthetic Doppler spectroscopy and curvilinear camera diagnostics in the ERO code. Computer Physics Communications, 2013, 184, 1842-1847.	7.5	1
178	Measurement of N+ flows in the high-field side scrape-off layer of ASDEX upgrade with different degrees of inner divertor detachment. Nuclear Materials and Energy, 2017, 12, 935-941.	1.3	1